Blood Flow Simulation of Left Ventricle with Twisted Motion

Masashi Yamakawa[1], Yuto Yoshimi[1], Shinichi Asao[2] and Seiichi Takeuchi[2]

[1] Faculty of Mechanical Engineering, Kyoto Institute of Technology, Japan
[2] Department of Mechanical Engineering, College of Industrial Technology, Japan
yamakawa@kit.ac.jp

Abstract. To push out a blood flow to an aorta, a left ventricle repeats expansion and contraction motion. For more efficient pumping of the blood, it is known that the left ventricle also has twisted motion. In this paper, the influence of the twisted motion for a blood flow to an aorta was investigated. In particular, the relationship between the origin of cardiovascular disease and wall shear stress has been pointed out in the aorta region. Estimating the difference of the wall shear stress depend on the presence or absence of the twisted motion, the blood flow simulation was conducted. To express its complicated shape and the motion, the unstructured moving grid finite volume method was adopted. In this method, the control volume is defined for a space time unified domain. Not only a physical conservation law but also a geometric conservation law is satisfied in this approach. Then high accurate computation is conducted under the method. From the computation results, a remarkable difference of complicated vortex structures generated in the left ventricle was found as the influence of the left ventricular twisted motion. The vortex structures affected the blood flow leading into the aorta with the result that they generated a clear difference of the wall shear stress. The region where the difference occurred is aortic arch, then it corresponded with a favorite site of arteriosclerosis. Thus, the result showed the possibility that the simulation with the left ventricular twisted motion would be useful to specify causes of heart diseases.

Keywords: Computational fluid dynamics, Blood flow simulation, Left ventricle, Aorta, Twisted motion.

1 Introduction

Serious disorders directly associated with the cause of death, for example arteriosclerosis or aneurism, are seen in a heart and vascular diseases. Then, the relation between the origin of the heart disease and blood flow has been pointed out. To specify causes of the diseases, flows in a heart or blood vessel have been studied through the method of experimentation or numerical simulation. Ku et al. [1] made a measurement the intimal thickening generated at the branching part of the human arteria carotis communis, as they were focused on the relations between the intimal thickening of an artery and the blood flow. Then, it was shown that the intimal thickening has a correlation with

ICCS Camera Ready Version 2022
To cite this paper please use the final published version:
DOI: 10.1007/978-3-031-08760-8_29

the time fluctuation of shear stress measured on a glass tube flow made from specimens of blood vessel. Fukushima et al. [2] created a visualization of blood flow using the real blood vessel taken out from the body. The real blood vessel is made transparent by salicylic acid. Then, they determined whether vortex tube exist at the bifurcation of the blood vessel. While, Oshima et al. [3] have developed the simulation system the M-SPhyR to achieve multi scale and physics simulation. The system integrates image-based modeling, blood-borne material and interaction between blood flows and blood vessel walls. Using the system, they calculated the blood flows in the arterial circle of Willis as the cardinal vascular network of the brain. Then, they have succeeded to recreate the collateral flow which is an important function at the flow control depended on the arterial circle of Willis.

From the geometric view, the aorta connected to the left ventricle is comprised of three parts as the aorta ascendens expanding upward, the aortic arch taking a bend, and the aorta descendens expanding downward. Then, the three principal branched blood vessels expand from the aortic arch. While, the motion of the left ventricle are not only expansion and contraction but also twisted motion [4]. The twisted motion like wring a left ventricle can pump out blood efficiently, then the ejection fraction touches 70 percent despite the cardiac fiber's contraction factor of 20 percent. As the pumping mechanism of the left ventricle is gathering attention from engineering field, it is executing novel ideas regarding an industrial pump with twisted motion. Thus, the motion of the left ventricle wall is very interesting in terms of medical and engineering field [5].

It is easy to assume that a difference of left ventricular motion affects a blood flow not only in the left ventricle but also in the aorta. Then, the difference of the blood flow would affect the risk and favorite site of a cardiac disease. In this paper, the pulsatile flows at the left ventricle and the aorta are computed and estimated using the left ventricular movement with twisted motion. In particular, to satisfy a physical conservation law and a geometric conservation law, the unstructured moving grid finite volume method [6-7] is adopted. In this method, a control volume is defined for a space time unified domain. The method made it possible to compute accurately for motion of the left ventricle and the aorta. Furthermore, the unstructured mesh approach was also able to express such the complicated shape. Then, the computation was carried out under the OpenMP parallel environment [8].

2 Numerical Approach

2.1 Governing Equations

As governing equations, the continuity equation and the Navier-Stokes equations for incompressible flows are adopted and written as follows:

$$\nabla \cdot \mathbf{q} = 0, \tag{1}$$

ICCS Camera Ready Version 2022
To cite this paper please use the final published version:
DOI: 10.1007/978-3-031-08760-8_29

$$\frac{\partial \boldsymbol{q}}{\partial t}+\frac{\partial \boldsymbol{E}_a}{\partial x}+\frac{\partial \boldsymbol{F}_a}{\partial y}+\frac{\partial \boldsymbol{G}_a}{\partial z}= -\left(\frac{\partial \boldsymbol{E}_p}{\partial x}+\frac{\partial \boldsymbol{F}_p}{\partial y}+\frac{\partial \boldsymbol{G}_p}{\partial z}\right)+\frac{1}{\mathrm{Re}}\left(\frac{\partial \boldsymbol{E}_v}{\partial x}+\frac{\partial \boldsymbol{F}_v}{\partial y}+\frac{\partial \boldsymbol{G}_v}{\partial z}\right), \tag{2}$$

where $\boldsymbol{q}$ is the velocity vector, $\boldsymbol{E}_a$, $\boldsymbol{F}_a$, and $\boldsymbol{G}_a$ are advection flux vectors in the x, y, and z direction, respectively, $\boldsymbol{E}_v$, $\boldsymbol{F}_v$, and $\boldsymbol{G}_v$ are viscous-flux vectors, and $\boldsymbol{E}_p$, $\boldsymbol{F}_p$, and $\boldsymbol{G}_p$ are pressure terms. The elements of the velocity vector and flux vectors are

$$\begin{gathered}\boldsymbol{q}=\begin{bmatrix}u\\v\\w\end{bmatrix},\ \boldsymbol{E}_a=\begin{bmatrix}u^2\\uv\\uw\end{bmatrix},\ \boldsymbol{F}_a=\begin{bmatrix}uv\\v^2\\vw\end{bmatrix},\ \boldsymbol{G}_a=\begin{bmatrix}uw\\vw\\w^2\end{bmatrix},\ \boldsymbol{E}_p=\begin{bmatrix}p\\0\\0\end{bmatrix},\\ \boldsymbol{F}_p=\begin{bmatrix}0\\p\\0\end{bmatrix},\ \boldsymbol{G}_p=\begin{bmatrix}0\\0\\p\end{bmatrix},\ \boldsymbol{E}_v=\begin{bmatrix}\partial u/\partial x\\\partial v/\partial x\\\partial w/\partial x\end{bmatrix},\ \boldsymbol{F}_v=\begin{bmatrix}\partial u/\partial y\\\partial v/\partial y\\\partial w/\partial y\end{bmatrix},\ \boldsymbol{G}_v=\begin{bmatrix}\partial u/\partial z\\\partial v/\partial z\\\partial w/\partial z\end{bmatrix},\end{gathered} \tag{3}$$

where u, v, and w are the velocity components of the x, y, and z directions, respectively, and p is pressure. Re is the Reynolds number.

2.2 The Unstructured Moving-Grid Finite-Volume Method

In this simulation, expansion and contraction of the left ventricle and translation motion of the aorta are expressed using moving mesh approach. To assure a geometric conservation law in moving mesh, a control volume is defined in a space-time unified domain. For the discretization, Eq. (2) can be written in divergence form as

$$\tilde{\nabla}\cdot\tilde{\mathbf{F}}=\mathbf{0}, \tag{4}$$

where

$$\tilde{\nabla}=\begin{bmatrix}\frac{\partial}{\partial x}\\\frac{\partial}{\partial y}\\\frac{\partial}{\partial z}\\\frac{\partial}{\partial t}\end{bmatrix},\quad \tilde{\mathbf{F}}=\begin{bmatrix}\mathbf{E}_a+\mathbf{E}_p-\frac{1}{\mathrm{Re}}\mathbf{E}_v\\\mathbf{F}_a+\mathbf{F}_p-\frac{1}{\mathrm{Re}}\mathbf{F}_v\\\mathbf{G}_a+\mathbf{G}_p-\frac{1}{\mathrm{Re}}\mathbf{G}_v\\\mathbf{q}\end{bmatrix}. \tag{5}$$

ICCS Camera Ready Version 2022
To cite this paper please use the final published version:
DOI: 10.1007/978-3-031-08760-8_29

The flow variables are defined at the center of the cell in the (x, y, z) space, as the approach is based on a cell-centered finite volume method. Thus, the control volume becomes a four-dimensional polyhedron in the (x, y, z, t)-domain. For the control volume, Eq. (4) is integrated using the Gauss theorem and written in surface integral form as:

$$\int_{\tilde{\Omega}} \tilde{\nabla} \cdot \tilde{\boldsymbol{F}} \mathrm{d}\tilde{V} = \oint_{\partial\tilde{\Omega}} \tilde{\boldsymbol{F}} \cdot \tilde{\boldsymbol{n}}_u \mathrm{d}\tilde{S} \approx \sum_{l=1}^{6} \left(\tilde{\boldsymbol{F}} \cdot \tilde{\boldsymbol{n}} \right)_l = \boldsymbol{0} \tag{6}$$

Here, $\tilde{\mathbf{n}}_u$ is an outward unit vector normal to the surface, $\partial\tilde{\Omega}$, of the polyhedron control volume $\tilde{\Omega}$, and $\tilde{\mathbf{n}} = (\tilde{n}_x, \tilde{n}_y, \tilde{n}_z, \tilde{n}_t)_l$, ($l$=1, 2,... 6) denotes the surface normal vector of control volume, and its length is equal to the boundary surface area in four-dimensional (x, y, z, t) space. The upper and bottom boundary of the control volume (l = 5 and 6) are perpendicular to the t-axis, and therefore they have only the $\tilde{n}_t$ component, and its length corresponds to the volume of the cell in the (x, y, z)-space at time t^n and t^{n+1}, respectively.

3 Computational Model and Conditions

3.1 Geometric Model of Left Ventricle and Aorta

A main function of the left ventricle is pumping blood to an aorta. The mitral valve and the aortic valve are put in the inlet and the outlet of the ventricle, respectively. The shape of the left ventricle is shown in Fig. 1. Bothe of the diameter of blood vessels at the mitral valve and the aortic valve are 3.0cm. The length from the base of heart to the cardiac apex is 7.8cm at lumen maximum volume. The cross-section shape of the left ventricle is ellipse. Then, the ratio of the major axis and minor axis on the ellipse is 5 to 4.

While, the aorta is comprised of three parts which are the ascending aorta expanding upward, the aortic arch taking a bend, and the descending aorta expanding downward. Furthermore, the three principal branched blood vessels which are called innominate artery, left common carotid artery and left subclavian artery expand from the aortic arch. Then the aortic arch itself curves three-dimensionally. In other words, the central axis of the aortic arch in not on a plane surface. Thus, the aorta is complicated shape with bending, bifurcation and three-dimensional torsion. In this paper, the shape of the aorta model is created, as shown Fig. 2.

ICCS Camera Ready Version 2022
To cite this paper please use the final published version:
DOI: 10.1007/978-3-031-08760-8_29

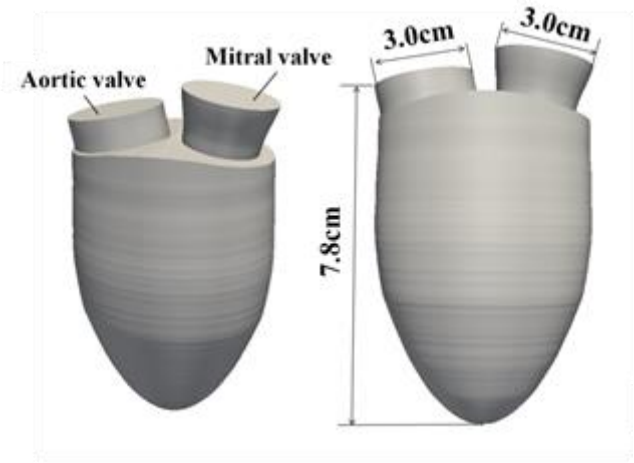

Fig. 1. Left ventricle model.

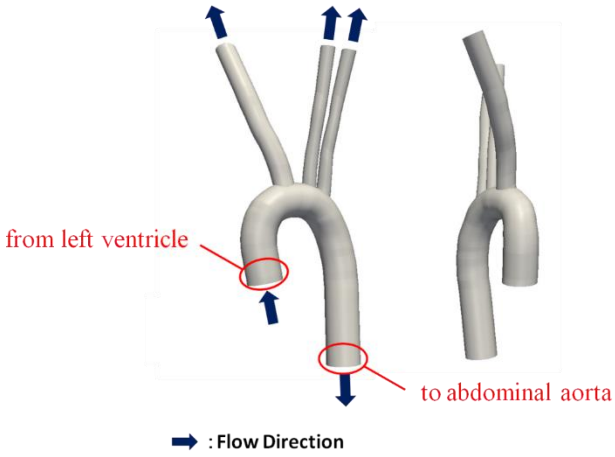

Fig. 2. Aorta model.

3.2 Motions of Left Ventricle and Aorta

The left ventricle is draining blood to the aorta by expansion and contraction. Then the heart rate is determined the systole and diastole of the heart. Then, a period from starting point to the next starting point of heart rate is called the cardiac cycle. If a pulse rate is 60bpm, one cardiac cycle would be 1.0sec. Then, it is classified 0.49sec as the systole and 0.51sec as the diastole. The history of the left ventricle cavity volumetric change in one cardiac cycle is shown in Fig. 3. The expansion and contraction using moving mesh at the simulation are expressed under the history.

In addition, the left ventricle has a twisted motion for effective pumping. In this paper, the influence of the twisted motion for a flow in the aorta is investigated with

ICCS Camera Ready Version 2022
To cite this paper please use the final published version:
DOI: 10.1007/978-3-031-08760-8_29

comparing with and without twisted motion. The case without twisted motion has just inward motion (contraction –expansion movement), as shown in Fig.4. On the other hand, the case with twisted motion has torsion movement around its vertical axis in addition to inward motion, as shown in Fig. 5. In this case, the maximum torsion angle at base of heart is 3 degrees. Then, the maximum torsion angle at apex of heart is 7.8 degrees. These twist in the opposite direction respectively.

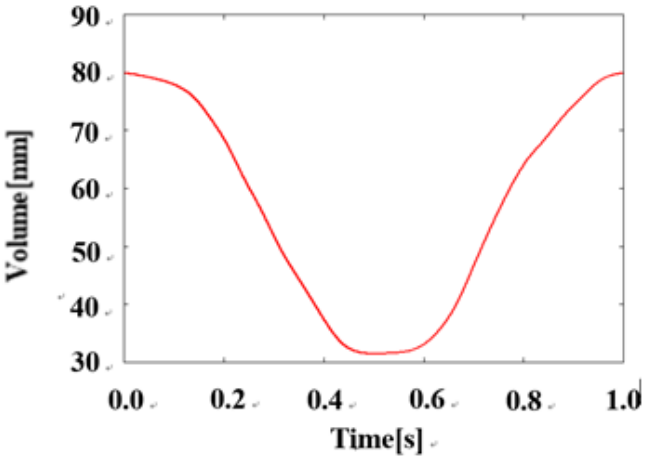

Fig. 3. History of left ventricle volumetric change.

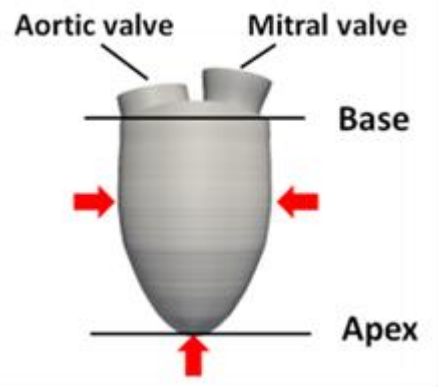

Fig. 4. Image of inward motion of the left ventricle (Case 1).

ICCS Camera Ready Version 2022
To cite this paper please use the final published version:
DOI: 10.1007/978-3-031-08760-8_29

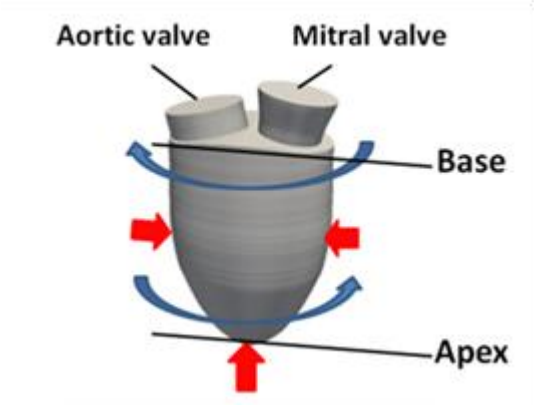

Fig. 5. Image of twisted motion in addition to inward motion (Case 2).

The computation models with/without twisted motion at the minimum volume of the heart are compared in Fig. 6. Here, the twisted motion is confirmed by the vertical blue line in the figure. History of volume change in both cases are same. Difference of both cases are just shear stress for circumferential direction. Furthermore, translational motion [9-10] for the left ventricle and the aorta is also adopted in this simulation.

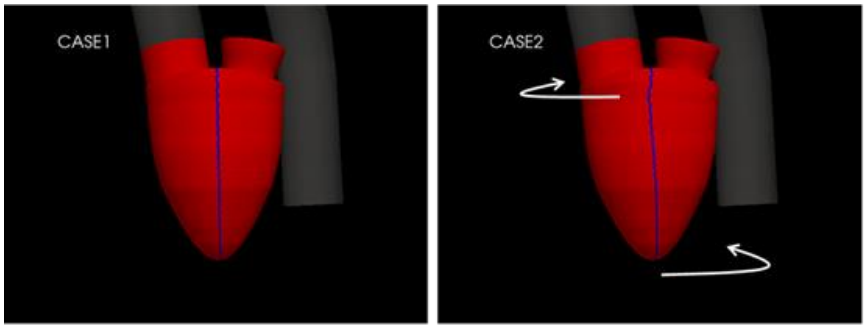

Fig. 6. Comparison of twisted motion by vertical blue line

3.3 Computational Conditions

The computational mesh is generated by MEGG3D [11] using tetrahedral and prism elements, as shown in Fig. 7. MEGG3D is a mesh generation software provided by Japan Aerospace Exploration Agency. The number of elements for the left ventricle model is 1,145,432 (tetrahedron: 755,042, prism: 390,390) and for the aorta is 1,631,657 (tetrahedron: 856,386, prism: 775,271). Then, the total number of the elements are 2,777,089.

ICCS Camera Ready Version 2022
To cite this paper please use the final published version:
DOI: 10.1007/978-3-031-08760-8_29

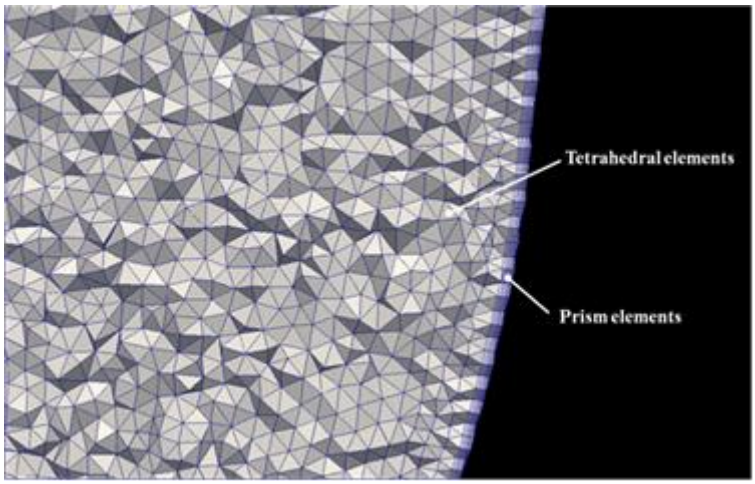

Fig. 7. Computational mesh near the wall

The heart rate is 60bpm, and the Reynolds number is 2,030. As an initial condition, pressure $p = 0$ and velocity for x, y, z directions $u = v = w = 0$ are obtained for all elements. In the cardiac diastole, the mitral valve is open and the aortic valve is closed completely. Then, the velocity at the mitral valve is given as a linear extrapolation and pressure is fixed as $p = 0$. While, in the cardiac systole, the mitral valve is closed and the aortic valve is open completely. These open and closing motions are conducted instantly. On the four exit of blood vessels, velocity is determined as a linear extrapolation and pressure is zero. The velocity on all walls of the left ventricle and the aorta is given the moving velocity decided expansion, contraction, translational motion and twisted motion.

4 Computational Results

4.1 Comparison of flows in the left ventricle

Fig. 8 shows isosurface of Q-criterion in left ventricle at $t = 23.0$, 25.0 and 27.0. Here, the simulation starts at the beginning of diastolic phase. Then, one cycle (diastole and systole) is 10.0 as dimensionless time. Thus, the figure ($t = 23.0$, 25.0 and 27.0) is in third diastolic and systolic phase. There are some vortices generated by pulsation until second phase in the left ventricle. To the vortices area, ring vortex tube flow through the mitral valve is seen at $t = 23.0$. Then, the vortex tube becomes disrupted according to decline of blood inflow from the mitral valve, expanding to inside of the left ventricle with complicated eddy structure.

ICCS Camera Ready Version 2022
To cite this paper please use the final published version:
DOI: 10.1007/978-3-031-08760-8_29

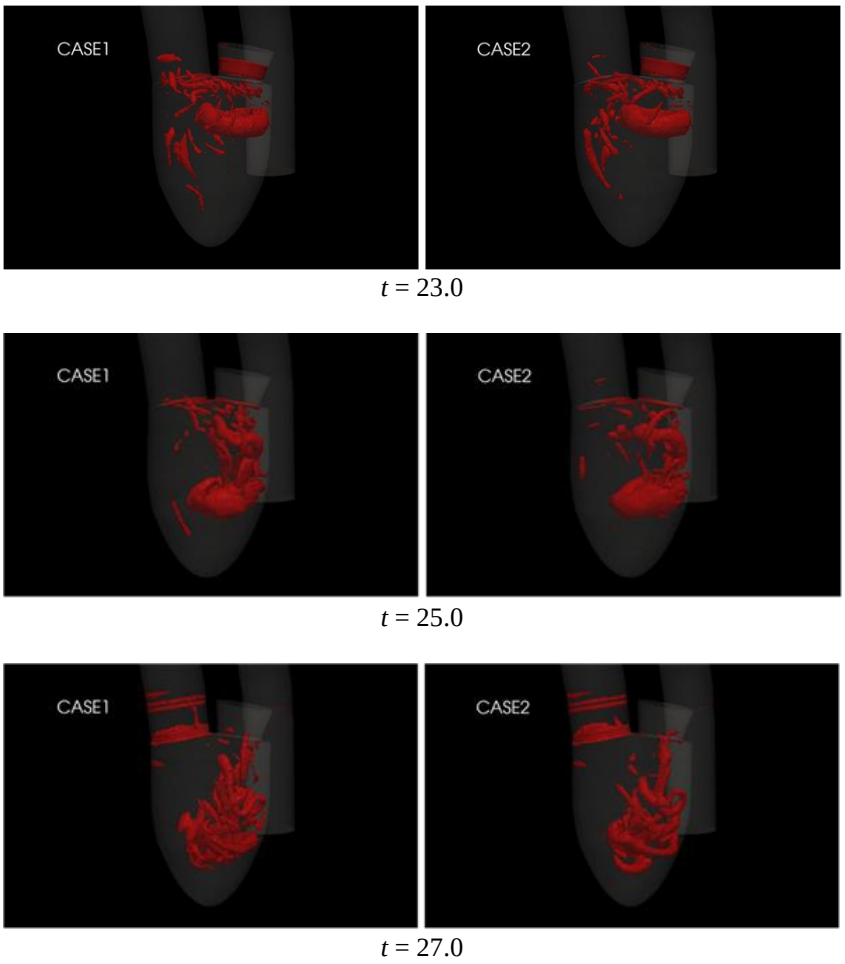

Fig. 8. Isosurface of Q-criterion in left ventricle (t = 23.0, 25.0, 27.0)
(Case1: inward motion, Case2: inward and twisted motion)

In Fig. 8, the flow phenomenon between by inward motion (left: case1) and by inward + twisted motion (right: case2) should show the same trend. However, the detail eddy structures are markedly different. The difference is caused by addition of the twisted motion. Then, the difference should affect to flows in an aorta.

4.2 Shear stress on the wall of aorta

To investigate the influence of flows caused by twisted motion of left ventricle, a flow in an aorta is simulated. Fig. 9 shows shear stress on the wall of the aorta at t = 25.0, 27.0 and 29.0. They are in the systolic phase. The systole starts at t =25.0. Thus, there is little wall shear stress at t =25.0. At mid of systole (t = 27.0), a large change in a

ICCS Camera Ready Version 2022
To cite this paper please use the final published version:
DOI: 10.1007/978-3-031-08760-8_29

direction and a magnitude of wall shear stress is seen. It should be caused by complicated flow in the aorta.

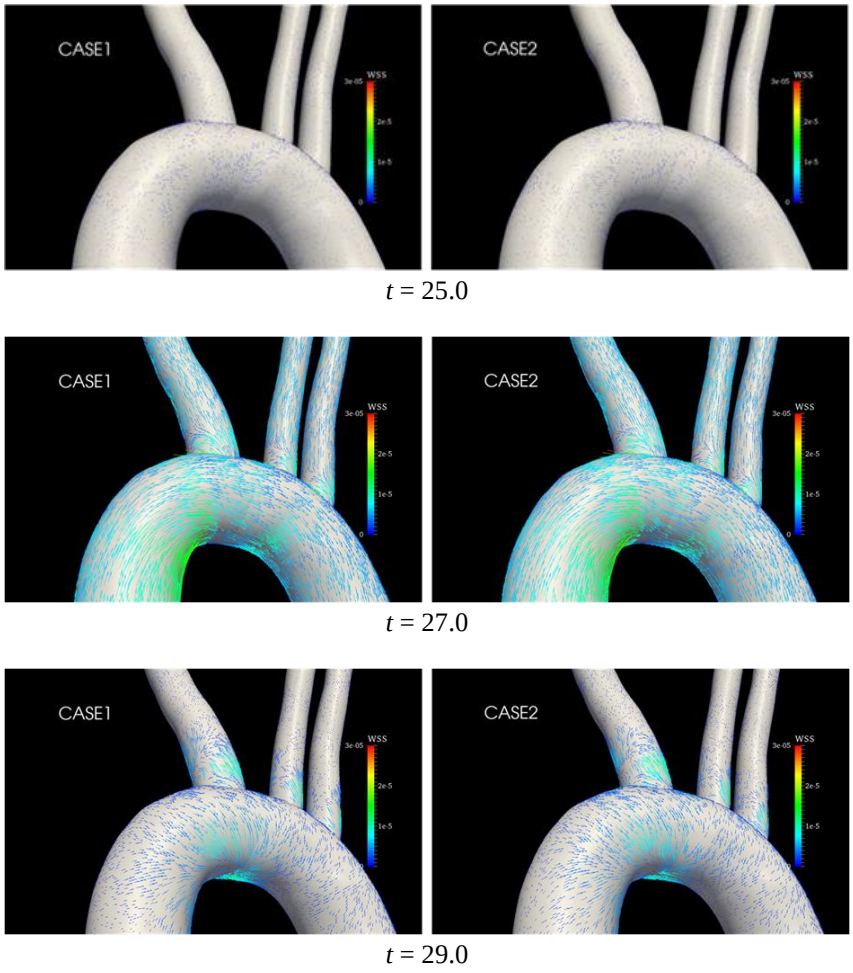

Fig. 9. Shear stress on the wall of aorta (t = 25.0, 27.0, 29.0)
(Case1: inward motion, Case2: inward and twisted motion)

From mid to end in systole at t = 29.0, we can see that the direction of wall shear stress reverses with mainstream at a part of the aortic arc. It is also confirmed from pressure contours of the left ventricle and aorta at t = 27.0 and 29.0, as shown in Fig. 10. It should be caused by decreasing of inner pressure of the left ventricle.

Here, Ku [1] reported that there is correlative relationship between rate of back stream of wall shear stress on the aorta for mainstream and the intimal thickening which is early involvement of atherosclerosis. On the other hand, it is known that an aortic arc is favorite site of arteriosclerosis. Thus, the simulation result which shows back stream of wall shear stress for mainstream is validity from a medical field.

ICCS Camera Ready Version 2022
To cite this paper please use the final published version:
DOI: 10.1007/978-3-031-08760-8_29

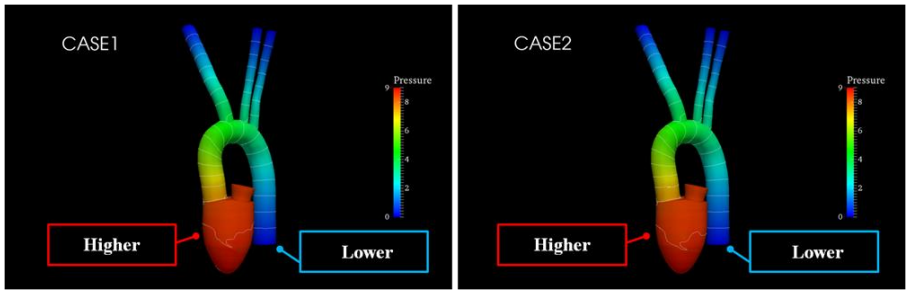

t = 27.0

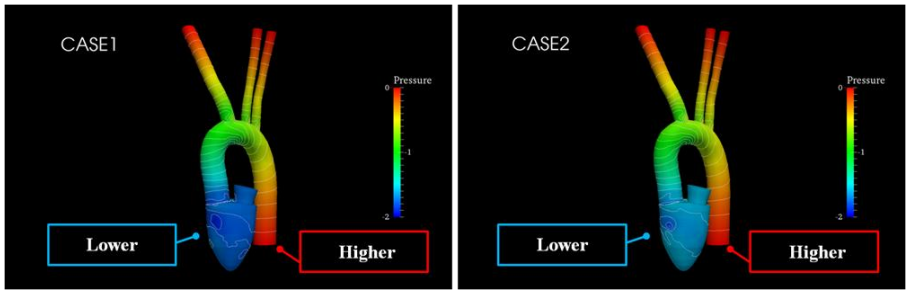

t = 29.0

Fig. 10. Pressure contours on the left ventricle and aorta (t = 27.0 and 29.0) (Case1: inward motion, Case2: inward and twisted motion)

Although there is a slight difference between just inward motion and additional twisted motion on pressure contours at t = 29.0, there is almost no difference in both on other pressure contours and distribution of wall shear stress of aorta. To clarify the difference of influence on the aorta by flows from left ventricle, time averaged wall shear stress of the aorta in third systolic phase are shown in Fig. 11. Then, Fig. 12 shows difference between time averaged wall shear stress decided by inward motion and shear stress by additional twisted motion (difference between case1 and case2). As the figure, clear differences are seen at the bifurcation (Location 1) and at the bottom of aortic arc (Location 2). It means that the difference of motions of left ventricle affects to the wall shear stress at the bifurcation and the bottom of aortic arc. The detail of the differences at the locations are shown in Table 1. We can see 17.9% difference of wall shear stress at the bifurcation (Location 1) and 6.2% difference of wall shear stress at the bottom of aortic arc (Location 2). These are great differences.

ICCS Camera Ready Version 2022
To cite this paper please use the final published version:
DOI: 10.1007/978-3-031-08760-8_29

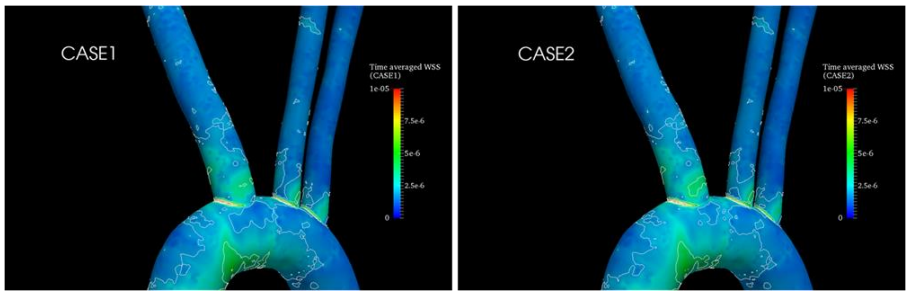

Fig. 11. Time averaged wall shear stress in third systolic phase (Case1: inward motion, Case2: inward and twisted motion)

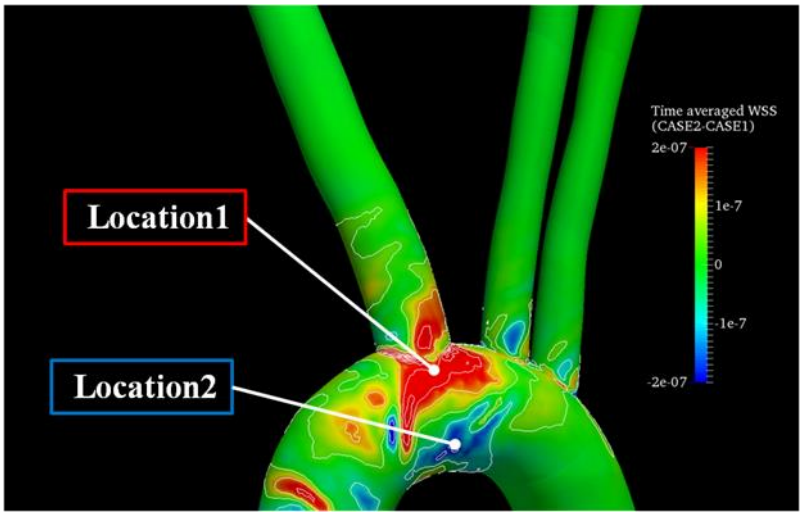

Fig. 12. Difference of time averaged wall shear stress for Case1 and Case2

Table 1. Comparison between time averaged wall shear stress for Case1 and Case2

	A	B	C	D	E
Location1	1.46×10^{-6}	1.72×10^{-6}	2.62×10^{-7}	17.9	1.18
Location2	3.29×10^{-6}	3.09×10^{-6}	-2.04×10^{-7}	6.18	0.94

A : Time averaged wall shear stress for Case1 (dimensionless quantity)
B : Time averaged wall shear stress for Case2 (dimensionless quantity)
C : For Case2 – For Case1 (dimensionless quantity)
D : {|For Case2 – For Case1|/For Case1}×100[%]
E : For Case2/For Case1

ICCS Camera Ready Version 2022
To cite this paper please use the final published version:
DOI: 10.1007/978-3-031-08760-8_29

As these results, we confirmed that motions of left ventricle affect to flows in the ventricle, and the flows also influence in the aorta. More than 10% difference of wall shear stress in the aorta caused by the twisted motion was also confirmed. In this paper, we adopted just one small motion. In fact, there are a lot of complicated motions of the left ventricle. Thus, difference of real motions of left ventricle should affect to risk and favorite site of vascular lesions. Therefore, when individual risk of vascular lesion for patients is referred, it is important to focus motions of left ventricle.

5 Conclusions

To express the influence to behavior of blood flow in a left ventricle and an aorta by twisted motion of the left ventricle, flows in the left ventricle and the aorta were computed using moving mesh method. First, it was shown that different motion between inward and additional twisted motion affect to the detail eddy structures in the left ventricle. From mid to end in systole, the reverse flow of wall shear stress for mainstream at a part of the aortic arc was seen. The correspondence of the result with the medical knowledge showed the validity of the simulation. Furthermore, more than 10% difference of wall shear stress in the aorta caused by the twisted motion was also confirmed. Although just twisted motion was adopted in this paper, there are a lot of complicated motions of the left ventricle in practical. Thus, difference of real motions of left ventricle should affect to risk and favorite site of vascular lesions. Therefore, when individual risk of vascular lesion for patients is referred, it is important to focus motions of left ventricle.

Acknowledgments

This publication was subsidized by JKA through its promotion funds from KEIRIN RACE.

References

1. Ku, D., Giddens, et al, (1985) Pulsatile flow and atherosclerosis in the human carotid bifurcation. Positive correlation between plaque location and low oscillating shear stress., Arteriosclerosis Vol.5, 293-302
2. Fukushima, T. et al. (1982) The horseshoe vortex: A secondary flow generated in arteries with stenosis, bifurcation, and branching, Biorheology Vol.19, 143-154.
3. Oshima, M. et al. (2007) Multi-Scale & Multi-Physics Simulation of Cerebrovascular Disorders, Journal of Japan Society of Fluid Mechanics, 26(6), 369-374
4. Omar, A. M. et al. (2015) Left ventricular twist and torsion, Circulation: Cardio-vascular Imaging, Aug;8(8) e000009.
5. Liang, F., et al. (2007) A multi-scale computational method applied to the quantitative evaluation of the left ventricular function, Computers in Biology and Medicine, Vol.37, 700-715

ICCS Camera Ready Version 2022
To cite this paper please use the final published version:
DOI: 10.1007/978-3-031-08760-8_29

6. Yamakawa, M., et al. (2012) Numerical Simulation for a Flow around Body Ejection using an Axisymmetric Unstructured Moving Grid Method, Computational Thermal Sciences, Vol.4, No.3, 217-223.
7. Yamakawa, M., et al. (2017) Numerical Simulation of Rotation of Intermeshing Rotors using Added and Eliminated Mesh Method, Procedia Computer Science 108C, 1883-1892.
8. Yamakawa, M., et al. (2011) Domain decomposition method for unstructured meshes in an OpenMP computing environment, Computers & Fluids, Vol. 45, pp.168-171.
9. Yamakawa, M. et al. (2019) Blood flow simulation of left ventricle and aorta with translation motion, The Proc. of the International Conference on Computational Methods, Vol.6, pp.7-17
10. Fukui, T., et al. (2017) Influence of geometric changes in the thoracic aorta due to arterial switch operations on the wall shear stress distribution, Open Biomedical Engineering Journal, 11, 9-16.
11. Ito, Y. (2013) Challenges in Unstructured Mesh Generation for Practical and Efficient Computational Fluid Dynamics Simulations, Computers and Fluids, 85, 47-52.

ICCS Camera Ready Version 2022
To cite this paper please use the final published version:
DOI: 10.1007/978-3-031-08760-8_29